

# Pharmacophoric Search and 3D-QSAR Comparative Molecular Field Analysis Studies on Agonists of Melatonin Sheep Receptors

Christophe Marot,<sup>\*,†</sup> Philippe Chavatte,<sup>‡</sup> Luc Morin-Allory,<sup>†</sup> Marie Claude Viaud,<sup>†</sup> Gérald Guillaumet,<sup>†</sup> Pierre Renard,<sup>§</sup> Daniel Lesieur,<sup>‡</sup> and André Michel<sup>||</sup>

*Institut de Chimie Organique et Analytique, associé au CNRS, Université d'Orléans, BP 6759, 45067 Orléans Cedex 2, France, Institut de Chimie Pharmaceutique, 3 rue du Professeur Laguesse, BP 83, 59006 Lille, France, ADIR et Cie., 1 rue Carle Hébert, 92415 Courbevoie, France, and Institut de Recherches SERVIER, 11 rue des Moulineaux, 92150 Suresnes, France*

Received January 14, 1998

Conformational analysis was used to characterize the agonist pharmacophore for melatonin sheep brain receptor recognition and activation. The molecular geometry shared by all conformations of the selected active ligands was determined. Assuming that all the compounds interact at the same binding site at the receptor level, 2-iodomelatonin pharmacophoric conformation served as a template for the superimposition of 64 structurally heterogeneous agonists constituting the training set used to perform a three-dimensional quantitative structure–activity relationship study via the comparative molecular field analysis method. A statistically significant model was obtained for the totality of the compounds ( $n = 64$ ,  $q^2 = 0.62$ ,  $N = 6$ ,  $r^2 = 0.96$ ,  $s = 0.28$ ,  $F = 249$ ) with steric, electrostatic, and lipophilic relative contributions of 28%, 35%, and 37%, respectively. The predictive power of the proposed model was discerned by successfully testing the 78 agonist ligands constituting the test set. The model so obtained and validated brings important structural insights to aid the design of novel melatonergic agonist ligands prior to their synthesis.

## Introduction

Melatonin (*N*-acetyl-5-methoxytryptamine) (Figure 1) is an hormone principally synthesized and secreted by the pineal gland.<sup>1</sup> Tryptophan is taken up by the pinealocyte and transformed to serotonin which is then converted into melatonin via a two-step biochemical pathway.<sup>2</sup> Its production is regulated by a circadian rhythm related to the photoperiodic environment. Melatonin circulating levels reach maximum values in the middle of the night and slowly decrease to minimal values in the morning. Melatonin appears to play a central role in the control of circadian rhythms in humans. It is involved in sleep regulation as well as in various endocrine and immune functions.<sup>3</sup> In addition, melatonin might exert protective effects on the cardiovascular system<sup>4</sup> and might slow the processes of aging by acting as a free radicals scavenger.<sup>5,6</sup> These numerous effects suggest potential therapeutic applications for melatonin such as sleep disorders, jet lag, shift work syndrome, seasonal affective disorders, blindness, and aging.<sup>7</sup> However, the use of melatonin as a drug is limited by its short half-life (15–20 min), its poor oral bioavailability, and its ubiquitous action. To solve this problem, several compounds that display more favorable metabolic and pharmacological properties than the lead structure have been synthesized. Their design was based on bioisosteric modifications of the indole ring and on pharmacomodulation of the *N*-acylamino and methoxy groups. Since the first cloning of a melatonin

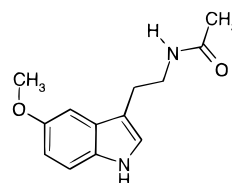


Figure 1. Molecular structure of melatonin.

receptor from *Xenopus* dermal melanophores,<sup>8</sup> several members of the mammalian and vertebrate family have been cloned and classified within three receptors subtypes referred to as Mel<sub>1a</sub>, Mel<sub>1b</sub>, and Mel<sub>1c</sub>.<sup>9</sup> Mel<sub>1a</sub> and Mel<sub>1b</sub> subtypes have been cloned from human tissue, sequenced, and shown to be members of the G protein-coupled superfamily of receptors. Mel<sub>1a</sub> receptor, which has been found in the hypophyseal pars tuberalis and in the hypothalamic SCN, might mediate the circadian and reproductive actions of melatonin while Mel<sub>1b</sub> receptor, which has been found in retina might mediate the effects of melatonin in the retina.<sup>8</sup> However, their tridimensional structure is unknown, and we have considered available agonist ligands which bind at the same site in order to define the common geometry shared by all of them. Then, we have used this putative pharmacophoric information to analyze the relationship between a large number of structurally heterogeneous agonists of the sheep brain melatonin receptor and their affinities using the comparative molecular field analysis (CoMFA) method based on steric, electrostatic, and lipophilic fields.<sup>10,11</sup> The predictive power of the model allows it to turn into a valuable tool to aid the design of novel melatonergic agonist ligands prior to their synthesis.

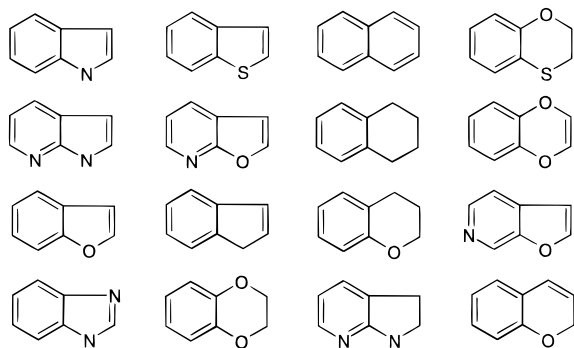
\* To whom correspondence should be addressed.

<sup>†</sup> Université d'Orléans.

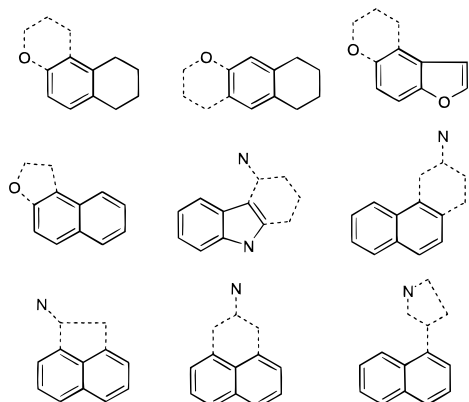
<sup>‡</sup> Institut de Chimie Pharmaceutique.

<sup>§</sup> ADIR et Cie.

<sup>||</sup> Institut de Recherches SERVIER.



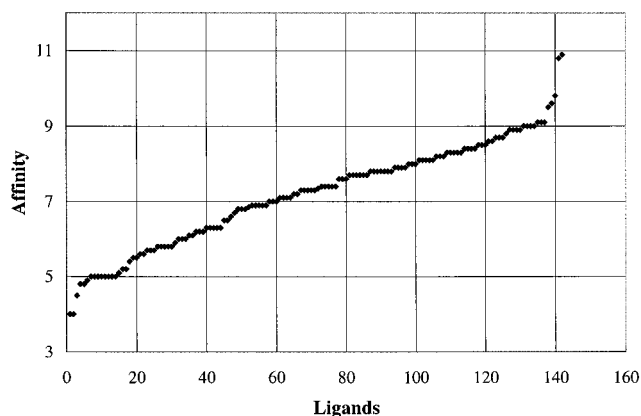
**Figure 2.** Definition of the 16 classes of tensors of ligands investigated in this study.



**Figure 3.** Conformationally constrained structures.

## Materials and Methods

**Selection of Ligands.** The binding affinity values for the melatonin receptor of 300 compounds found in the literature<sup>12–20</sup> and in our laboratory database were compiled and critically evaluated. All values retained had been determined by binding studies using 2-[<sup>125</sup>I]-iodomelatonin on ovine pars tuberalis membrane homogenates<sup>2</sup> and are expressed as shown in Tables 1–16 for the 142 selected compounds in terms of pIC<sub>50</sub>. Agonist activity of these ligands was evaluated by measuring the melatonin-mediated inhibition of forskolin-stimulated cAMP production.<sup>21,22</sup> The retained compounds belong to 16 structurally different families depending on the tensor aryl moiety (Figure 2). These tensors were indole, pyrrolopyridine, benzofurane, benzodioxane, furopyridine, indene, benzothiophene, naphthalene, tetraline, chromane, thiochromane, benzodioxine, and benzoxathiine derivatives, and most of them contain the highly flexible ethylamido side chain and alkoxy group on the aryl moiety. However, in some cases, the ethylamido side chain and the methoxy group are conformationally constrained (Figure 3). Their receptor binding affinities are spread out over a wide range in a homogeneous fashion (Figure 4). Of the 142 compounds selected, 35 display pIC<sub>50</sub> values less than 6 (no affinity), 24 display pIC<sub>50</sub> values between 6 and 7 (very low affinity), 43 exhibit pIC<sub>50</sub> values between 7 and 8 (low affinity), and 40 show pIC<sub>50</sub> values higher than 8 (good affinity). The great structural diversity and the homogeneous repartition of the affinities are necessary to obtain meaningful results from a three-dimensional quantitative structure–activity relationships (3D-QSAR) study using the CoMFA method.<sup>10,11</sup>



**Figure 4.** Distribution of affinity of all ligands investigated.

**Table 1.** pIC<sub>50</sub> Values for the Compounds of the Training Set

compd	R1	R2	R3	pIC <sub>50</sub>
<b>8</b>	–OCH <sub>2</sub> COOH	–(CH <sub>2</sub> ) <sub>2</sub> NHCOCH <sub>3</sub>	–H	5.8
<b>17</b>	–OCH <sub>2</sub> CH <sub>3</sub>	–(CH <sub>2</sub> ) <sub>2</sub> NHCOCH <sub>3</sub>	–H	6.9
<b>20</b>	–OCH <sub>3</sub>	–(CH <sub>2</sub> ) <sub>2</sub> NHCONH(CH <sub>2</sub> ) <sub>2</sub> CH <sub>3</sub>	–H	7.1
<b>34</b>	–OCH <sub>3</sub>	–(CH <sub>2</sub> ) <sub>2</sub> NHSO <sub>2</sub> CH <sub>3</sub>	–H	7.9
<b>39</b>	–OCH <sub>3</sub>	–(CH <sub>2</sub> ) <sub>2</sub> NHCONHCH <sub>2</sub> CH <sub>3</sub>	–H	8.1
<b>43</b>	–OCH <sub>3</sub>	–(CH <sub>2</sub> ) <sub>2</sub> NHCO–cyclopropyl	–H	8.3
<b>48</b>	–OCH <sub>3</sub>	–(CH <sub>2</sub> ) <sub>2</sub> NHCONHCH <sub>3</sub>	–H	8.5
<b>54</b>	–OCH <sub>3</sub>	–(CH <sub>2</sub> ) <sub>2</sub> NHCOCH <sub>3</sub>	–H	8.8
<b>63</b>	–OCH <sub>3</sub>	–(CH <sub>2</sub> ) <sub>2</sub> NHCOCH <sub>3</sub>	–CH <sub>2</sub> Ph	10.8

**Table 2.** pIC<sub>50</sub> Values for the Compounds of the Training Set

compd	R1	R2	pIC <sub>50</sub>
<b>19</b>	–CH <sub>2</sub> CH <sub>3</sub>	–(CH <sub>2</sub> ) <sub>2</sub> NHCONHCH <sub>3</sub>	7
<b>21</b>	–CH <sub>2</sub> CH <sub>3</sub>	–(CH <sub>2</sub> ) <sub>2</sub> NHCOCH <sub>2</sub> CH <sub>3</sub>	7.2
<b>23</b>	–O(CH <sub>2</sub> ) <sub>2</sub> CH <sub>3</sub>	–(CH <sub>2</sub> ) <sub>2</sub> NHCOCH <sub>3</sub>	7.6

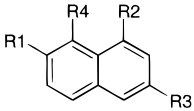
**Table 3.** pIC<sub>50</sub> Values for the Compounds of the Training Set

compd	R1	R2	R3	R4	pIC <sub>50</sub>
<b>4</b>	–H	–H	–H	–(CH <sub>2</sub> ) <sub>2</sub> NHCOCH <sub>3</sub>	5
<b>18</b>	–OCH <sub>3</sub>	–(CH <sub>2</sub> ) <sub>2</sub> NHCOCH <sub>3</sub>	–H	–H	6.9
<b>64</b>	–OCH <sub>3</sub>	–(CH <sub>2</sub> ) <sub>2</sub> NHCOCH <sub>3</sub>	–Ph	–H	10.9

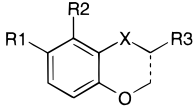
**Table 4.** pIC<sub>50</sub> Values for the Compounds of the Training Set

compd	R1	R2	pIC <sub>50</sub>
<b>24</b>	–OCH <sub>3</sub>	–(CH <sub>2</sub> ) <sub>2</sub> NHCONH(CH <sub>2</sub> ) <sub>2</sub> CH <sub>3</sub>	7.7
<b>57</b>	–OCH <sub>3</sub>	–(CH <sub>2</sub> ) <sub>2</sub> NHCOCH <sub>3</sub>	9
<b>59</b>	–OCH <sub>3</sub>	–(CH <sub>2</sub> ) <sub>2</sub> NHCOCH <sub>3</sub>	9.1

To carry out this study, we have used a training set containing 64 compounds (Tables 1–7) and a test set of 78 compounds (Tables 8–16) in order to assess the

**Table 5.** pIC<sub>50</sub> Values for the Compounds of the Training Set


compd	R1	R2	R3	R4	pIC <sub>50</sub>
2	-OCH <sub>3</sub>	-(CH <sub>2</sub> ) <sub>2</sub> NHCO(CH <sub>2</sub> ) <sub>5</sub> CH <sub>3</sub>	-H	-H	4
6	-OCH <sub>3</sub>	-(CH <sub>2</sub> ) <sub>2</sub> NHCO(CH <sub>2</sub> ) <sub>4</sub> CH <sub>3</sub>	-H	-H	5.7
12	-H	-(CH <sub>2</sub> ) <sub>2</sub> NHCONH <sub>2</sub>	-H	-H	6.3
13	-OCH <sub>3</sub>	-(CH <sub>2</sub> ) <sub>3</sub> NHCONH(CH <sub>2</sub> ) <sub>2</sub> CH <sub>3</sub>	-H	-H	6.6
14	-OCH <sub>3</sub>	-(CH <sub>2</sub> ) <sub>2</sub> NHCO-cyclopropyl	-COCH <sub>3</sub>	-H	6.9
22	-OCH <sub>3</sub>	-(CH <sub>2</sub> ) <sub>2</sub> NHCONH(CH <sub>2</sub> ) <sub>2</sub> CH <sub>3</sub>	-H	-H	7.3
25	-O(CH <sub>2</sub> ) <sub>5</sub> CH <sub>3</sub>	-(CH <sub>2</sub> ) <sub>2</sub> NHCOCH <sub>3</sub>	-H	-H	7.7
26	-OCH <sub>3</sub>	-(CH <sub>2</sub> ) <sub>3</sub> CONH <sub>2</sub>	-H	-H	7.7
27	-OCH <sub>3</sub>	-CH(CH <sub>2</sub> OH)CH <sub>2</sub> NHCOCH <sub>3</sub>	-H	-H	7.7
28	-OCH <sub>3</sub>	-(CH <sub>2</sub> ) <sub>2</sub> NHCOCH <sub>3</sub>	-CH <sub>2</sub> Ph	-H	7.8
29	-O(CH <sub>2</sub> ) <sub>3</sub> CH <sub>3</sub>	-(CH <sub>2</sub> ) <sub>2</sub> NHCOCH <sub>2</sub> CH <sub>3</sub>	-H	-H	7.8
32	-OCH <sub>3</sub>	-(CH <sub>2</sub> ) <sub>2</sub> CONHCH <sub>3</sub>	-H	-H	7.9
33	-OCH <sub>3</sub>	-(CH <sub>2</sub> ) <sub>2</sub> NHCSNHCH <sub>3</sub>	-H	-H	7.9
35	-OCH <sub>2</sub> CH=CH <sub>2</sub>	-(CH <sub>2</sub> ) <sub>2</sub> NHCO-cyclopropyl	-H	-H	7.9
37	-OCH <sub>3</sub>	-(CH <sub>2</sub> ) <sub>2</sub> NHCONHCH <sub>2</sub> CH <sub>3</sub>	-H	-H	8
38	-OCH <sub>3</sub>	-CH <sub>2</sub> ONHCOCH <sub>3</sub>	-H	-H	8.1
40	-OCH <sub>2</sub> -cyclopropyl	-(CH <sub>2</sub> ) <sub>2</sub> NHCOCH <sub>2</sub> CH <sub>3</sub>	-H	-H	8.1
41	-OCH <sub>3</sub>	-(CH <sub>2</sub> ) <sub>2</sub> NHCOCH <sub>3</sub>	-(CH <sub>2</sub> ) <sub>2</sub> CH <sub>3</sub>	-H	8.2
42	-O(CH <sub>2</sub> ) <sub>4</sub> CH <sub>3</sub>	-(CH <sub>2</sub> ) <sub>2</sub> NHCOCH <sub>2</sub> CH <sub>3</sub>	-H	-H	8.2
44	-OCH <sub>2</sub> C≡CH	-(CH <sub>2</sub> ) <sub>2</sub> NHCOCH <sub>3</sub>	-H	-H	8.3
45	-OCH <sub>3</sub>	-CH(OH)CH <sub>2</sub> NHCOCH <sub>3</sub>	-H	-H	8.3
46	-OCH <sub>3</sub>	-(CH <sub>2</sub> ) <sub>2</sub> NHCONH <sub>2</sub>	-H	-H	8.4
47	-OCH <sub>3</sub>	-CH <sub>2</sub> ONHCO(CH <sub>2</sub> ) <sub>2</sub> CH <sub>3</sub>	-H	-H	8.4
49	-OH	-(CH <sub>2</sub> ) <sub>2</sub> NHCOCH <sub>2</sub> CH <sub>3</sub>	-H	-CH <sub>2</sub> CH=CH <sub>2</sub>	8.5
50	-OCH <sub>3</sub>	-(CH <sub>2</sub> ) <sub>2</sub> NHCO-isopropyl	-H	-H	8.6
51	-OCH <sub>3</sub>	-(CH <sub>2</sub> ) <sub>2</sub> NHCONHCH <sub>3</sub>	-H	-H	8.6
52	-OCH <sub>2</sub> CH=CH <sub>2</sub>	-(CH <sub>2</sub> ) <sub>2</sub> NHCOCH <sub>2</sub> CH <sub>3</sub>	-H	-H	8.7
53	-OCH <sub>3</sub>	-(CH <sub>2</sub> ) <sub>2</sub> NHCOCH <sub>2</sub> CH <sub>3</sub>	-H	-H	8.7
56	-OCH <sub>3</sub>	-(CH <sub>2</sub> ) <sub>2</sub> NHCO-cyclopropyl	-H	-H	8.9
58	-OCH <sub>2</sub> CH <sub>3</sub>	-(CH <sub>2</sub> ) <sub>2</sub> NHCOCH <sub>3</sub>	-H	-H	9.1
60	-OCH <sub>2</sub> CH <sub>3</sub>	-(CH <sub>2</sub> ) <sub>2</sub> NHCOCH <sub>2</sub> CH <sub>3</sub>	-H	-H	9.1

**Table 6.** pIC<sub>50</sub> Values for the Compounds of the Training Set


compd	R1	R2	R3	X		pIC <sub>50</sub>
5	-OCH <sub>3</sub>	-H	-NHCOCH <sub>3</sub>	-CH <sub>2</sub>	single	5
9	-H	-H	-(CH <sub>2</sub> ) <sub>2</sub> NHCOCH <sub>3</sub>	-O	double	6
10	-OCH <sub>3</sub>	-H	-(CH <sub>2</sub> ) <sub>2</sub> NHCOCH <sub>3</sub>	-O	single	6.1
11	-H	-O(CH <sub>2</sub> ) <sub>3</sub> NHCOCH <sub>3</sub>	-H <sub>2</sub>	-O	single	6.2
15	-H	-(CH <sub>2</sub> ) <sub>3</sub> NHCOCH <sub>3</sub>	-H <sub>2</sub>	-O	single	6.9
16	-H	-(CH <sub>2</sub> ) <sub>4</sub> NHCOCH <sub>3</sub>	-H <sub>2</sub>	-S	single	6.9
30	-H	-(CH <sub>2</sub> ) <sub>3</sub> CONHCH <sub>3</sub>	-H <sub>2</sub>	-O	single	7.8

predictive power of the model. These sets have been created in order to contain compounds of all the families. In each family, compounds have been split between training and test sets in a random way.

**Conformational Analysis.** Molecular modeling studies were performed using SYBYL software version 6.2<sup>23</sup> running on Silicon Graphics workstations. Three-dimensional models of all compounds were built from a standard fragments library, and their geometry was subsequently optimized using the Tripos force field<sup>24</sup> including the electrostatic term calculated from Gasteiger and Hückel atomic charges. The method of Powell available in the Maximin2 procedure was used for energy minimization until the gradient value was smaller than 0.001 kcal/mol Å<sup>2</sup>. For each compound, a conformational search using the random search process as implemented in SYBYL was performed to identify

its lowest energy conformations. Random conformational searching is a technique to locate energy minima of a molecule. It involves making random torsion changes to selected bonds, followed by a minimization. The cycle of random changes and minimization is repeated many times. After each cycle the new conformation is compared against all others found so far to see if it is unique. For the random search, the main options used are the maximum hits ( $n = 10$ ) which defined the minimum number of times each conformation must be found to stop searching for new conformations, the RMS threshold (root-mean-square (RMS) = 0.2 Å) which defined the maximum RMS difference between two conformations before they are considered different, the energy cutoff ( $E =$  energy obtained after minimization + 20 kcal/mol) which defined the maximum allowable energy for a conformation, and the

**Table 7.** pIC<sub>50</sub> Values for the Compounds of the Training Set

compd	structure	pIC <sub>50</sub>
1		4
3		5
7		5.8
31		7.8
36		8
55		8.9
61		9.6
62		9.8

**Table 8.** pIC<sub>50</sub> Values for the Compounds of the Test Set

compd	R1	R2	R3	pIC <sub>50</sub>
84	-(CH <sub>2</sub> ) <sub>2</sub> CH <sub>3</sub>	-(CH <sub>2</sub> ) <sub>2</sub> NHCOCH <sub>3</sub>	-H	5.8
104	-OCH <sub>3</sub>	-(CH <sub>2</sub> ) <sub>2</sub> NHSO <sub>2</sub> CH <sub>2</sub> CH <sub>3</sub>	-H	7
107	-O-isopropyl	-(CH <sub>2</sub> ) <sub>2</sub> NHCOCH <sub>3</sub>	-H	7.1
111	-O(CH <sub>2</sub> ) <sub>3</sub> CH <sub>3</sub>	-(CH <sub>2</sub> ) <sub>2</sub> NHCOCH <sub>3</sub>	-H	7.3
116	-OCH <sub>3</sub>	-(CH <sub>2</sub> ) <sub>2</sub> NHCOCH <sub>2</sub> CH <sub>3</sub>	-CH <sub>2</sub> Ph	7.4
120	-OCH <sub>3</sub>	-(CH <sub>2</sub> ) <sub>2</sub> NHCOCH <sub>3</sub>	-H	7.6
122	-OCH <sub>3</sub>	-(CH <sub>2</sub> ) <sub>2</sub> NHCOCH <sub>2</sub> Br	-H	7.7
124	-OCH <sub>2</sub> C≡CH	-(CH <sub>2</sub> ) <sub>2</sub> NHCOCH <sub>3</sub>	-H	7.8
129	-OCH <sub>3</sub>	-(CH <sub>2</sub> ) <sub>2</sub> NHCOCH <sub>2</sub> I	-H	8.1
130	-OCH <sub>3</sub>	-(CH <sub>2</sub> ) <sub>2</sub> NHCO(CH <sub>2</sub> ) <sub>3</sub> CH <sub>3</sub>	-H	8.2

**Table 9.** pIC<sub>50</sub> Values for the Compounds of the Test Set

compd	R1	R2	R3	R4	pIC <sub>50</sub>
75	-H	-(CH <sub>2</sub> ) <sub>2</sub> NHCO(CH <sub>2</sub> ) <sub>3</sub> CH <sub>3</sub>	-H	-H	5.2
76	-H	-(CH <sub>2</sub> ) <sub>2</sub> NHCO-cyclopentyl	-H	-H	5.2
77	-H	-(CH <sub>2</sub> ) <sub>2</sub> NHCO-cyclobutyl	-H	-H	5.4
83	-H	-(CH <sub>2</sub> ) <sub>2</sub> NHCO(CH <sub>2</sub> ) <sub>6</sub> CH <sub>3</sub>	-H	-H	5.7
113	-OCH <sub>3</sub>	-(CH <sub>2</sub> ) <sub>2</sub> NHCONH(CH <sub>2</sub> ) <sub>2</sub> CH <sub>3</sub>	-H	-F	7.3
136	-OCH <sub>3</sub>	-(CH <sub>2</sub> ) <sub>2</sub> NHCO-cyclopropyl	-H	-F	8.7
138	-OCH <sub>3</sub>	-(CH <sub>2</sub> ) <sub>2</sub> NHCOCH <sub>2</sub> I	-H	-H	8.9
141	-OCH <sub>3</sub>	-(CH <sub>2</sub> ) <sub>2</sub> NHCOCH <sub>3</sub>	-I	-H	9

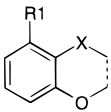
**Table 10.** pIC<sub>50</sub> Values for the Compounds of the Test Set

compd	R1	R2	pIC <sub>50</sub>
90	-CH <sub>2</sub> CH <sub>3</sub>	-(CH <sub>2</sub> ) <sub>2</sub> NHCONH(CH <sub>2</sub> ) <sub>2</sub> CH <sub>3</sub>	6.1
92	-CH <sub>2</sub> CH <sub>3</sub>	-(CH <sub>2</sub> ) <sub>2</sub> NHCO(CH <sub>2</sub> ) <sub>3</sub> CH <sub>3</sub>	6.2
93	-OCH <sub>3</sub>	-(CH <sub>2</sub> ) <sub>2</sub> NHCO(CH <sub>2</sub> ) <sub>3</sub> CH <sub>3</sub>	6.3
96	-H	-(CH <sub>2</sub> ) <sub>2</sub> NHCO-cyclobutyl	6.3
114	-OCH <sub>3</sub>	-(CH <sub>2</sub> ) <sub>2</sub> NHCO-cyclobutyl	7.4
131	-OCH <sub>3</sub>	-(CH <sub>2</sub> ) <sub>2</sub> NHCOCH <sub>2</sub> I	8.3
134	-OCH <sub>3</sub>	-(CH <sub>2</sub> ) <sub>2</sub> NHCO-cyclopropyl	8.4
137	-OCH <sub>3</sub>	-(CH <sub>2</sub> ) <sub>2</sub> NHCOCH <sub>3</sub>	8.9

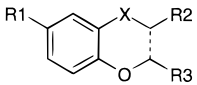
**Table 11.** pIC<sub>50</sub> Values for the Compounds of the Test Set

compd	R1	R2	R3	pIC <sub>50</sub>
66	-H	-H	-(CH <sub>2</sub> ) <sub>2</sub> NHCOCH <sub>3</sub>	single 4.8
68	-H	-(CH <sub>2</sub> ) <sub>2</sub> NHCOCH <sub>3</sub>	-H	double 4.9
80	-OCH <sub>3</sub>	-(CH <sub>2</sub> ) <sub>2</sub> NHCO-cyclopropyl	-CH <sub>3</sub>	double 5.6
95	-OCH <sub>3</sub>	-(CH <sub>2</sub> ) <sub>2</sub> NHCOCH <sub>3</sub>	-CH <sub>3</sub>	double 6.3

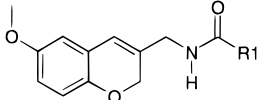
maximum cycles defined in comparison to the number of rotatable bonds. The conformations produced by the random conformational search are fully optimized and can be used immediately for further analysis. Among the so constituted conformational spaces, only the conformers with an energy of 10 kcal/mol above the lowest energy minima have been kept for their geometry

**Table 12.** pIC<sub>50</sub> Values for the Compounds of the Test Set


compd	R1	X	pIC <sub>50</sub>
69	-(CH <sub>2</sub> ) <sub>2</sub> CONHCH <sub>3</sub>	single -SO <sub>2</sub>	5
72	-CH <sub>2</sub> NHCOCH <sub>3</sub>	single -O	5
74	-O(CH <sub>2</sub> ) <sub>2</sub> NHCONH(CH <sub>2</sub> ) <sub>2</sub> CH <sub>3</sub>	single -O	5.1
78	-O(CH <sub>2</sub> ) <sub>2</sub> NHCOCH <sub>3</sub>	single -O	5.5
85	-O(CH <sub>2</sub> ) <sub>4</sub> NHCOCH <sub>3</sub>	single -O	5.8
94	-(CH <sub>2</sub> ) <sub>2</sub> NHCOCH <sub>3</sub>	single -O	6.3
101	-(CH <sub>2</sub> ) <sub>3</sub> NHCOCH <sub>3</sub>	single -S	6.8
102	-(CH <sub>2</sub> ) <sub>4</sub> NHCOCH <sub>3</sub>	single -O	6.8
112	-(CH <sub>2</sub> ) <sub>4</sub> CONHCH <sub>3</sub>	single -O	7.3
118	-(CH <sub>2</sub> ) <sub>3</sub> NHCO(CH <sub>2</sub> ) <sub>2</sub> CH <sub>3</sub>	double -O	7.4
127	-(CH <sub>2</sub> ) <sub>3</sub> CONHCH <sub>3</sub>	single -S	8

**Table 13.** pIC<sub>50</sub> Values for the Compounds of the Test Set


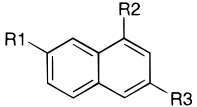
compd	R1	R2	R3	X	pIC <sub>50</sub>
65	-H	-CH <sub>2</sub> NHCOCH <sub>3</sub>	-Ph	-O double	4.5
71	-OCH <sub>3</sub>	-CH <sub>2</sub> NHCOCH <sub>3</sub>	-Ph	-O double	5
82	-H	-CH <sub>2</sub> NHCOCH <sub>3</sub>	-H <sub>2</sub>	-O single	5.7
88	-OCH <sub>3</sub>	-(CH <sub>2</sub> ) <sub>2</sub> NHCOCH <sub>3</sub>	-H <sub>2</sub>	-CH <sub>2</sub> single	6
117	-OCH <sub>3</sub>	-CH <sub>2</sub> NHCOCH <sub>3</sub>	-H <sub>2</sub>	-CH <sub>2</sub> single	7.4

**Table 14.** pIC<sub>50</sub> Values for the Compounds of the Test Set


compd	R1	pIC <sub>50</sub>
103	-CH <sub>3</sub>	4.8
123	-(CH <sub>2</sub> ) <sub>2</sub> CH <sub>3</sub>	7.7

reoptimization with the semiempirical MOPAC package version 6.0 using the Hamiltonian AM1.<sup>25</sup>

**Determination of the 3D Pharmacophore.** On the basis of several investigations of classical structure-activity relationships, the *N*-acetyl and 5-methoxy

**Table 15.** pIC<sub>50</sub> Values for the Compounds of the Test Set


compd	R1	R2	R3	pIC <sub>50</sub>
67	-OCH <sub>3</sub>	-CH <sub>2</sub> CONH(CH <sub>2</sub> ) <sub>3</sub> Ph	-H	4.8
87	-OCH <sub>3</sub>	-CONHCH <sub>3</sub>	-H	5.9
89	-OCH <sub>3</sub>	-(CH <sub>2</sub> ) <sub>2</sub> CONH <sub>2</sub>	-H	6
97	-O-cyclohexyl	-(CH <sub>2</sub> ) <sub>2</sub> NHCOCH <sub>3</sub>	-H	6.5
98	-H	-(CH <sub>2</sub> ) <sub>2</sub> NHCONHCH <sub>3</sub>	-H	6.5
99	-O(CH <sub>2</sub> ) <sub>2</sub> CH <sub>3</sub>	-(CH <sub>2</sub> ) <sub>2</sub> NHCO-cyclopropyl	-H	6.7
100	-OCH <sub>2</sub> COOH	-(CH <sub>2</sub> ) <sub>2</sub> NHCOCH <sub>3</sub>	-H	6.8
106	-OCH <sub>2</sub> CH <sub>3</sub>	-(CH <sub>2</sub> ) <sub>2</sub> NHCO-cyclobutyl	-H	7.1
110	-OCH <sub>3</sub>	-(CH <sub>2</sub> ) <sub>2</sub> NHCOCH <sub>3</sub>	-COCH <sub>2</sub> CH <sub>3</sub>	7.3
115	-OCH <sub>3</sub>	-(CH <sub>2</sub> ) <sub>2</sub> NHCOCH <sub>3</sub>	-CO-cyclopropyl	7.4
119	-OCH <sub>3</sub>	-(CH <sub>2</sub> ) <sub>2</sub> NHCOOCH <sub>3</sub>	-H	7.4
125	-OCH <sub>3</sub>	-(CH <sub>2</sub> ) <sub>2</sub> NHCO-cyclopropyl	-CH <sub>2</sub> CH <sub>3</sub>	7.8
128	-OCH <sub>3</sub>	-(CH <sub>2</sub> ) <sub>2</sub> NHCOCH <sub>3</sub>	-CH <sub>2</sub> -cyclopropyl	8.1
135	-O(CH <sub>2</sub> ) <sub>2</sub> CH <sub>3</sub>	-(CH <sub>2</sub> ) <sub>2</sub> NHCOCH <sub>2</sub> CH <sub>3</sub>	-H	8.5
142	-OCH <sub>3</sub>	-(CH <sub>2</sub> ) <sub>2</sub> NHCOCH <sub>3</sub>	-COPh	9.5

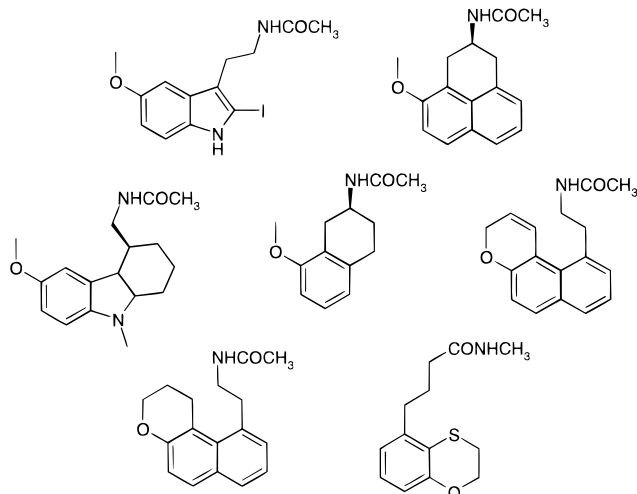
groups were defined as key elements of the melatonin-ergic agonist pharmacophore. Despite the lack of data concerning the three-dimensional structure of the melatonin-ergic receptor, the task was to identify conformational elements for each compound where these key pharmacophoric elements were spatially arranged in a way similar to that for a set of potent flexible or constrained ligands (Figure 5). The fitting attempts between the different conformers have been performed by using the "fit" option of SYBYL, and the quality of the superimposition was measured by the RMS value. In view of the considerable number of superimpositions to carry out for comparing the different conformers of each compound, the commonality was assessed by fitting molecular structural features chosen as the reference using an "in house" developed method written in SPL (SYBYL programming language). The cost in internal energy ( $\Delta E$ ) was estimated for each compound by comparing the energy of the putative pharmacophoric conformation to the energy of the most stable conformation. It is interesting to estimate the possibility for a molecule to exist in a clearly defined conformation in the binding site. For all the ligands, the cost in internal energy ( $\Delta E$ ) is always lower than 1 kcal/mol.

**Alignment of the Ligands.** One of the most important adjustable parameters in CoMFA is the relative alignment of all the ligands to one another in a way that they have a comparable conformation and a similar orientation in space. 2-Iodomelatonin pharmacophoric conformation (Figure 6) was used as template for the superimposition, assuming that all the compounds interact at the same binding site at the receptor level. Nine features were selected for the alignment of all ligands: the four atoms of the amido group, three atoms of the aromatic ring, and the two heavy atoms of the methoxy group. These atoms are numbered 1-9 in Figure 7. An example of this alignment is presented in Figure 8. The fitting process was performed using an "in house" developed method written in SPL. We have retained for each ligand the conformation with the best fit.

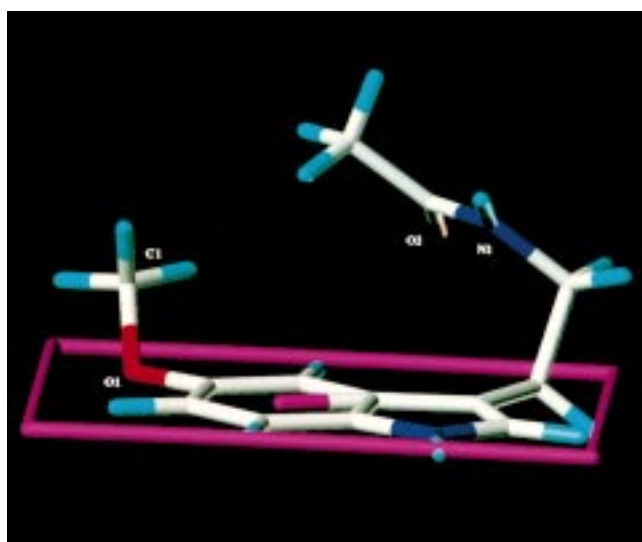
**Technical Specifications of the CoMFA Study.** The CoMFA studies were performed with the QSAR

**Table 16.** pIC<sub>50</sub> Values for the Compounds of the Test Set

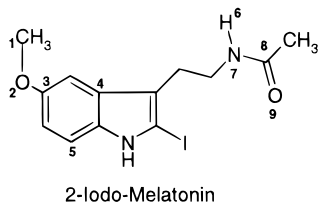
compd	structure	pIC <sub>50</sub>	compd	structure	pIC <sub>50</sub>
70		5	109		7.2
73		5	121		7.6
79		5.5	126		7.9
81		5.6	132		8.3
86		5.8	133		8.4
91		6.2	139		9
105		7	140		9
108		7.1			



**Figure 5.** Ligands selected for the pharmacophoric search.



**Figure 6.** Melatonergic pharmacophore. The folded structure of 2-iodomelatonin is characterized by several distances: the height of the amidic N-1 above the plane of the phenyl ring (2.4 Å); the height of the carbon C-1 of O-methoxy above the plane of the phenyl ring (1.1 Å); the distance between N-1 and O-1 (5.5 Å); the distance between O-2 and O-1 (5.1 Å); the distance between N-1 and the center of phenyl (4.2 Å); the distance between C-1 and the center of phenyl (3.6 Å).



**Figure 7.** Superposition modes.

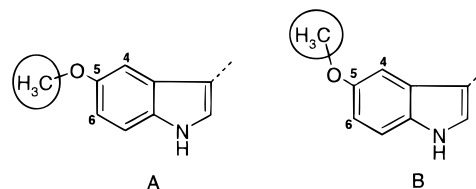
module of SYBYL for each combination of the three molecular fields: (S) steric, (E) electrostatic, and (L) lipophilic. The specific parameters used for CoMFA include a grid size of 1.5 Å and atomic charges recalculated with the semiempirical package MOPAC using the Hamiltonian AM1, a dielectric function of  $1/r$ , and a dielectric constant  $\epsilon = 1$ . We then used a  $sp^3$  carbon with a +1 charge as the probe in calculating the CoMFA potential at each point of the grid placed with 1.5 Å spacing. The lipophilic field was calculated by the



**Figure 8.** Alignment of three compounds *N*-[2-(2-iodo-5-methoxy-1*H*-3-indolyl)ethyl]acetamide, *N*-[(6-methoxy-9-methyl-2,3,4,9-tetrahydro-1*H*-4-carbazolyl)methyl]acetamide, and *N*-[4-methoxy-2,3-dihydro-1*H*-2-phenalenyl]acetamide.

**Table 17.** Color Code of Graphical CoMFA Results

field or component of field	increase affinity	decrease affinity
steric (S)	green	red
electrostatic (E)		
positive charge	white	magenta
negative charge	magenta	white
lipophilic (L)		
lipophilic component	yellow	cyan
hydrophilic component	cyan	yellow



**Figure 9.** Position of the methoxy group for (a) the pharmacophore of Sicsic et al.<sup>18</sup> and (b) our pharmacophore.

molecular lipophilic potential (MLP)<sup>26</sup> implemented in the CLIP<sup>27</sup> module of SYBYL. The method of partial least squares (PLS) implemented in the QSAR module of Tripos SYBYL V6.2 was employed to construct and validate the models. Cross-validation was performed with the leave-one-out procedure. The component number (*N*) retained for final PLS analyses corresponded to the first local maximum of the graph  $q^2 = f(N)$ . The other options were chosen according to published standards.<sup>28,29</sup>

**Presentation of the Results.** The graphical results in Figures 13–16 represent the most relevant regions of space where the variations of the statistical field are the largest. The color code used to characterize the signals of each field is described in Table 17. For the electrostatic field, a white zone can mean a favorable influence of some electron deficiency or an unfavorable influence of some high electron density. The interpretation of the lipophilicity field is similarly ambiguous. Indeed, lipophilicity encodes two major structural contributions,<sup>30</sup> namely, a bulk term reflecting hydrophobic and dispersive forces and a polar term reflecting more directional electrostatic interactions and hydrogen bonds.

**Table 18.** Statistical Results and CoMFA Models

models <sup>h</sup>	field type	q <sup>2</sup> <sup>a</sup>	N <sup>b</sup>	r <sup>2</sup> <sup>c</sup>	S <sup>d</sup>	F <sup>e</sup>	ster <sup>f</sup>	elec <sup>f</sup>	lipo <sup>f</sup>
A1	ster <sup>g</sup>	-0.06	1						
A2	elec <sup>g</sup>	0.00	1						
A3	lipo <sup>g</sup>	0.25	4						
A4	ster_elec	-0.01	1						
A5	ster_lipo	0.05	1						
A6	elec_lipo	0.16	6						
A7	ster_elec_lipo	0.05	1						
B1	ster	0.23	2						
B2	elec	0.25	3						
B3	lipo	0.45	4	0.93	0.37	114	100%		
B4	ster_elec	0.23	3						
B5	ster_lipo	0.37	3						
B6	elec_lipo	0.36	3						
B7	ster_elec_lipo	0.37	3						
C1	ster	0.56	2	0.92	0.33	30	100%		
C2	elec	-0.22	1						
C3	lipo	0.27	1						
C4	ster_elec	0.34	1						
C5	ster_lipo	0.40	1						
C6	elec_lipo	0.09	1						
C7	ster_elec_lipo	0.33	1						
D1	ster	0.22	3						
D2	elec	0.07	1						
D3	lipo	-0.18	1						
D4	ster_elec	0.20	3						
D5	ster_lipo	0.07	3						
D6	elec_lipo	-0.03	1						
D7	ster_elec_lipo	0.07	3						
E1	ster	0.41	2	0.85	1.02	21	100%		
E2	elec	0.41	2	0.89	0.86	32		100%	
E3	lipo	0.30	2						
E4	ster_elec	0.40	2						
E5	ster_lipo	0.32	2						
E6	elec_lipo	0.35	2						
E7	ster_elec_lipo	0.35	2						
F1	ster	0.49	3	0.92	0.32	39	100%		
F2	elec	0.46	3	0.95	0.26	63		100%	
F3	lipo	0.63	3	0.96	0.22	84			100%
F4	ster_elec	0.45	3	0.95	0.25	64	41%	59%	
F5	ster_lipo	0.59	3	0.96	0.24	72	41%		59%
F6	elec_lipo	0.59	2	0.95	0.25	101		48%	52%
F7	ster_elec_lipo	0.56	2	0.94	0.26	92	26%	36%	38%
G1	ster	0.41	3	0.8	0.64	82	100%		
G2	elec	0.44	5	0.9	0.47	100		100%	
G3	lipo	0.37	7						
G4	ster_elec	0.56	5	0.94	0.37	173	41%	59%	
G5	ster_lipo	0.46	4	0.89	0.49	115	41%		59%
G6	elec_lipo	0.51	6	0.96	0.3	215		48%	52%
G7	ster_elec_lipo	0.62	6	0.96	0.28	248	28%	35%	37%

<sup>a</sup> Cross-validation correlation coefficient. <sup>b</sup> Number of components used in final PLS analyses corresponded to the first maximum of the function  $q^2 = f(N)$  in cross-validation analyses. <sup>c</sup> Correlation coefficient of the final PLS analysis. <sup>d</sup> Standard error of estimate, measure of the unexplained uncertainty. <sup>e</sup> *F* ratio: the higher the *F* ratio, the better the PLS analysis. <sup>f</sup> Relative contribution of the steric (ster), electrostatic (elec), and lipophilic (lipo) field in the final PLS analysis. <sup>g</sup> Molecular field(s) used in 3D-QSAR CoMFA: ster = steric field, elec = electrostatic field, lipo = lipophilic field (calculated by MLP). <sup>h</sup> Model A (benzofurane-furopridine), model B (naphthalene), model C (benzothiophene), model D (tetraline-chromane-thiochromane), model E (indole-pyrrolopyridine-indene), model F (benzodioxine-benzoxathiine), model G (all compounds).

The favorable influence of the hydrophobic and hydrophilic components is described by yellow or cyan colors, respectively. By examining the moieties and functionalities involved, a chemist should be able to rely on common sense to remove the ambiguity in interpreting the influence of the electrostatic and lipophilicity fields.

## Results and Discussion

**Proposition of a Three-Dimensional Pharmacophore.** The aim of this study was the development of a 3D-QSAR agonist model which could accommodate a wide set of ligands with affinity for the sheep brain melatonin receptor. For this purpose, we have determined the geometry shared by all the constituent conformations of the conformational spaces of the

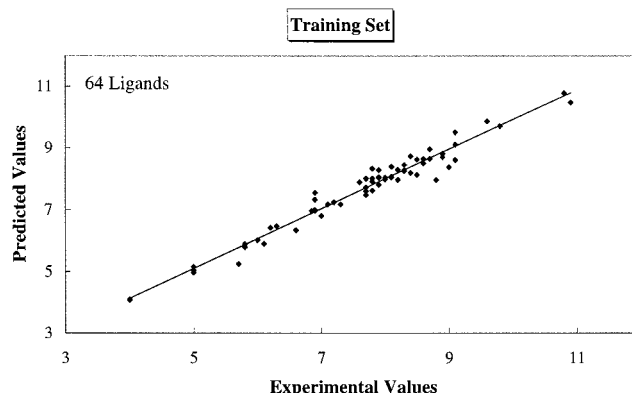
selected active ligands. If we consider that all the ligands bind at the same site at the receptor level, it is likely they adopt a common three-dimensional geometry that is responsible for their affinity and functional activity. This common geometry represents the bioactive conformation from which the pharmacophore will be defined. Only one type of pharmacophore emerged from this study as valid in terms of good fit evaluated by the RMS deviation between the relevant pharmacophoric atoms and reasonable energy compared with the lowest energy conformations. For each compound, it was possible to find stable conformations ( $\Delta E < 1$  kcal/mol) where the structural determinants were superimposed (RMS < 0.5 Å for active compounds). The biologically active conformation of a molecule is not



**Table 19.** Experimental vs Predicted  $pIC_{50}$  Values for the Training Set of Model G7

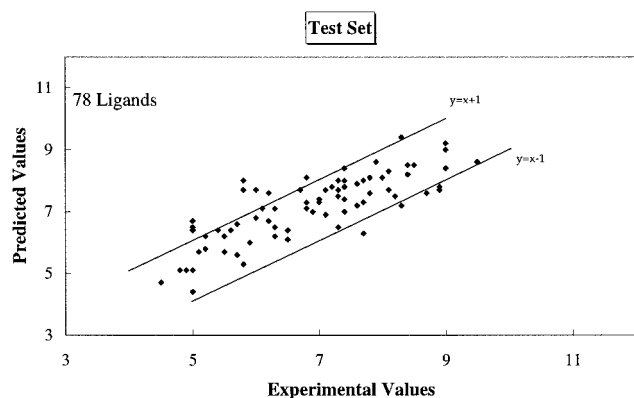
compd	exptl value	predct value	gap value	compd	exptl value	predct value	gap value	compd	exptl value	predct value	gap value	compd	exptl value	predct value	gap value
1	4.0	4.1	0.1	17	6.9	7.5	0.6	33	7.9	8.0	0.1	49	8.5	8.6	0.1
2	4.0	4.1	0.1	18	6.9	7.3	0.4	34	7.9	8.0	0.1	50	8.6	8.6	0
3	5.0	5.0	0	19	7.0	6.8	0.2	35	7.9	7.8	0.1	51	8.6	8.5	0.1
4	5.0	5.0	0	20	7.1	7.2	0.1	36	8.0	8.0	0	52	8.7	8.6	0.1
5	5.0	5.2	0.2	21	7.2	7.2	0	37	8.0	8.0	0	53	8.7	9	0.3
6	5.7	5.2	0.5	22	7.3	7.2	0.1	38	8.1	8.4	0.3	54	8.8	8.0	0.9
7	5.8	5.9	0.1	23	7.6	7.9	0.3	39	8.1	8.0	0.1	55	8.9	8.7	0.2
8	5.8	5.8	0	24	7.7	7.5	0.2	40	8.1	8.1	0	56	8.9	8.8	0.1
9	6.0	6.0	0	25	7.7	7.7	0	41	8.2	8.3	0.1	57	9.0	8.4	0.6
10	6.1	5.9	0.2	26	7.7	7.6	0.1	42	8.2	8.0	0.2	58	9.1	8.6	0.5
11	6.2	6.4	0.2	27	7.7	8.0	0.3	43	8.3	8.4	0.1	59	9.1	9.5	0.4
12	6.3	6.5	0.2	28	7.8	8.0	0.2	44	8.3	8.3	0	60	9.1	9.1	0
13	6.6	6.3	0.3	29	7.8	7.9	0.1	45	8.3	8.2	0.1	61	9.6	9.9	0.3
14	6.9	7.0	0.1	30	7.8	7.6	0.2	46	8.4	8.7	0.3	62	9.8	9.7	0.1
15	6.9	7.0	0.1	31	7.8	8.3	0.5	47	8.4	8.2	0.2	63	10.8	10.8	0
16	6.9	7.0	0.1	32	7.9	8.3	0.4	48	8.5	8.1	0.4	64	10.9	10.5	0.4

necessarily the one of lowest energy with regard to the capacity of the binding process to compensate the required increase in conformational energy. Thus, *N*-acetyl and methoxy groups of the different compounds can occupy the same relative position in space to interact with the melatonergic recognition site. Our melatonin agonist receptor pharmacophore may be described as 2-[I]iodomelatonin in a folded conformation and characterized by a set of distances as shown in Figure 6: the height of the amidic N-1 above the plane of the phenyl ring (2.4 Å), the height of the carbon C-1 of the methoxy group above the phenyl ring (1.1 Å), the distance between N-1 and O-1 (5.5 Å), the distance between O-2 and O-1 (5.1 Å), the distance between N-1 and the centroid of the phenyl ring (4.2 Å), and the distance between C-1 and the centroid of the phenyl ring (3.6 Å). Concerning the spatial position of the amidic group, this pharmacophore geometry is relatively consistent with that proposed recently by Sicsic et al.<sup>18</sup> who have carried out, in a very different approach, a conformational analysis based on the <sup>1</sup>H NMR study of a rigid agonist compound. However, our results do not agree with the spatial positions of the methoxy groups as shown in Figure 9. These authors have not taken into account the methyl orientation of the methoxy group which is important for the optimal orientation of the oxygen lone pairs with a view to obtain the best binding at the receptor level. Their pharmacophore seems to be in contradiction with previous SAR (structure–activity relationships)<sup>17</sup> studies which have shown that a cyclization between atoms C-5 and C-6 causes a decrease in affinity even when a cyclization between atoms C-4 and C-5 induces a consequent increase in affinity. In the same way, a chlorine substitution in position 6 forces the methoxy group to adopt a favorable orientation and leads to an increase in affinity. Ligands with the methoxy group involved in a cycle in the favorable position have been incorporated into the set of ligands selected for the pharmacophore search. In another way, Spadoni et al.<sup>31</sup> have more recently proposed two putative melatonergic pharmacophores determined from a study performed using the DISCO program with a set of judiciously chosen rigid ligands. They obtain models which are different from our own. As discussed above, the methoxy group for all ligands was also positioned in an arbitrary way. Furthermore, the two proposed models do not seem to correspond to

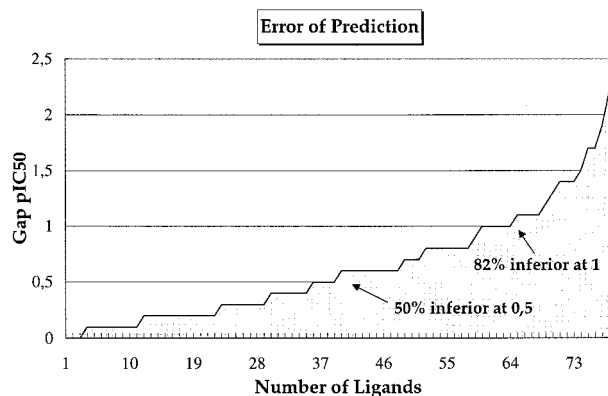
**Figure 10.**  $pIC_{50}$  values predicted by model G7 vs experimental values for the 64 compounds of the training set.

the bioactive conformation insofar as the compound *N*-[3-(2-carboxymethyl-5-methoxy-1*H*-indol-4-yl)propyl]-acetamide, which presents a flexible side chain, displays pharmacophoric geometries for the two proposed models and exhibits no affinity ( $pIC_{50} < 4$ ). The authors attempt to explain this contradiction by invoking the excessive flexibility of the molecule. Considering the affinity level ( $pIC_{50} > 10$ ) reached by some compounds of our training set (Tables 1–7), we assume that the presence of a highly flexible side chain is not incompatible with a very good affinity. On the contrary, this inactive compound is unable to fit properly the pharmacophoric features of our model as a result of the best measured fit RMS value (0.75 Å).

**Selection of the Best CoMFA Model.** After the ligands' alignment using the 2-iodomelatonin pharmacophoric conformation as template for the superimposition, we have carried out 49 different analyses according to the structural classes of ligands and the type of molecular field used in CoMFA. The classification of the ligands according to the chemical family in which they belong has yielded seven models: model A for benzofurane and furopyridine derivatives, model B only for naphthalene derivatives, model C for benzothiophene derivatives, model D for tetraline, chromane, and thiochromane derivatives, model E for indole, pyrrolopyridine, and indene derivatives, model F for benzodioxine, benzodioxane, and benzoxathiine derivatives, and finally, model G which combined the whole set of the compounds whatever their chemical class (64 com-



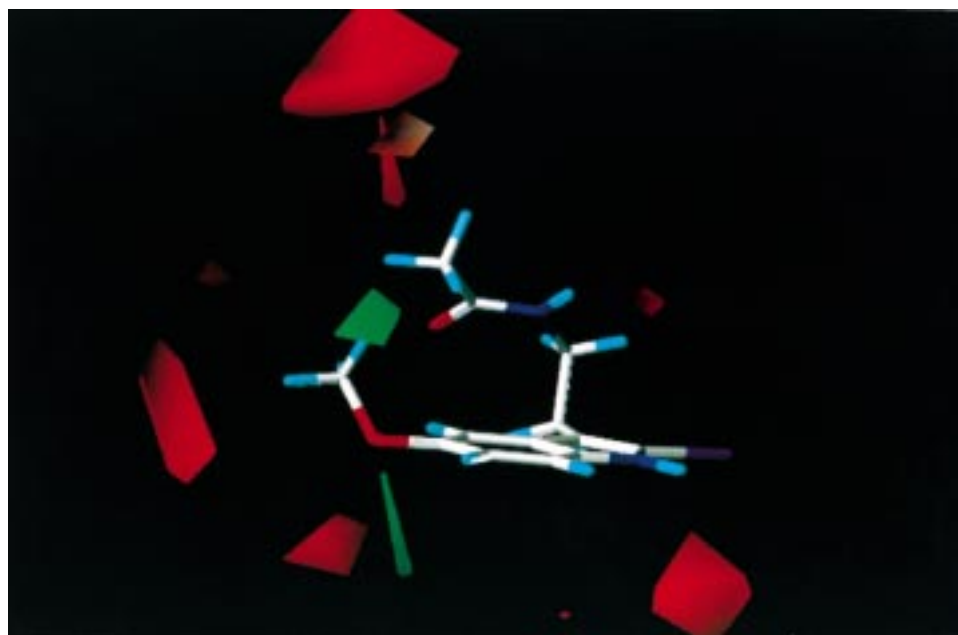
**Figure 11.**  $pIC_{50}$  values predicted by model G7 vs experimental values for the 78 compounds of the test set.



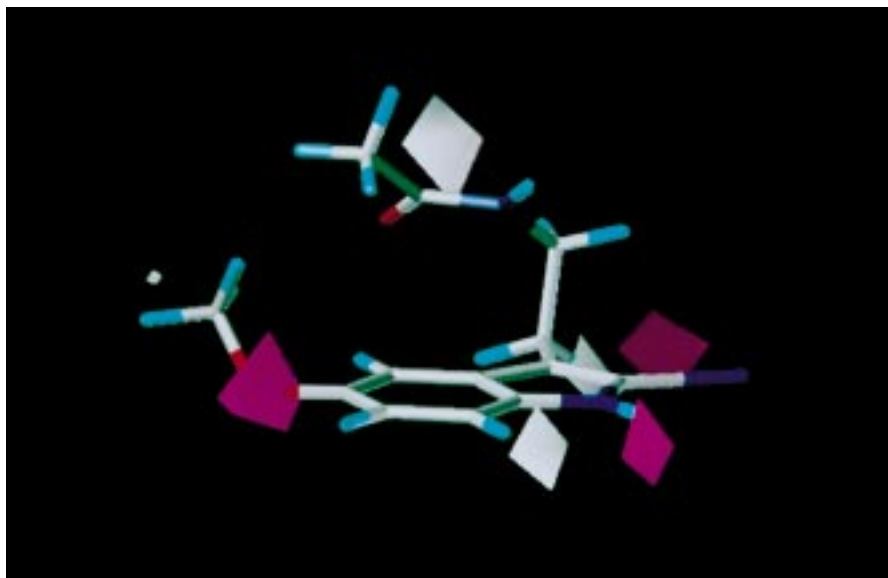
**Figure 12.** Gap between  $pIC_{50}$  values predicted by model G7 vs experimental values for the 78 compounds of the test set.

pounds) (Tables 1–7). For each model, the steric, electrostatic, and lipophilicity molecular fields were considered alone or in combination (Table 18). No PLS model with  $q^2 > 0.4$  was found for the models A and D. The number of compounds constituting these training sets was too limited and the structural variability in these series was too small to obtain a meaningful

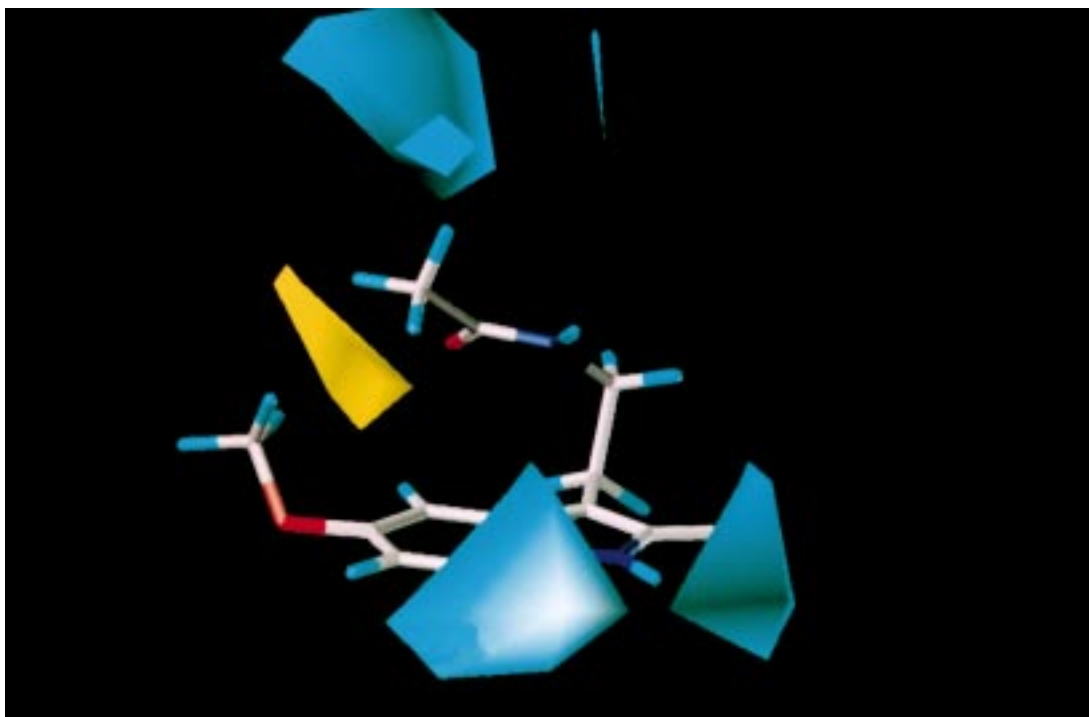
CoMFA model. For the model B, the best PLS model was obtained with only the lipophilic field, implying that the variability in this structural class is due exclusively to lipophilic factors. For model C, the variability was merely due to steric properties. But the accuracy of predictions obtained with these last two models was too poor to use them afterward. Regarding the model E, the variability might be explained either by steric factors or by electrostatic factors. In any case, the standard error of estimate which measures the unexplained uncertainty is too high to obtain a predictive model. Several good PLS models were found for model F, but the number of ligands was too limited and the structural variability of tensors in this series was too weak to obtain a usable CoMFA model. Then, we have studied the whole of the compounds corresponding to the model G. The best PLS analysis was obtained with the combination of steric, electrostatic and lipophilic fields ( $q^2 = 0.62$  and  $N = 6$ ). This model is statistically significant. A  $q^2$  value of 0.62 corresponds to a confidence limit superior at 95%, which minimizes the risk to find a correlation just by a mere chance. The number of components (6) is, moreover, weak considering the number of ligands present in the training set (64). This model G7 was the most predictive one according to the statistical results ( $r^2 = 0.96$ ,  $F = 248$ , and  $s = 0.28$ ). The estimated  $pIC_{50}$  values for the 64 compounds of the training set as well as residual values are given in Table 19, and the results are graphically represented in Figure 10. These data suggest a good correlation between the three molecular fields and the affinities registered for the different ligands. The relative contributions of each molecular field, steric (28%), electrostatic (35%), and lipophilic (37%), in our model G7 were practically equal. Graphical representations of this CoMFA model are displayed in Figures 13, 14, 15, and 16. They show regions where variations of a steric, electrostatic, or lipophilic nature in the structural features of the different molecules contained in the training set lead to increases or decreases in the affinity. In Figure 13,



**Figure 13.** Steric graphical results of PLS model G7 with 2-iodomelatonin (red = steric decrease affinity; green = steric increase affinity).



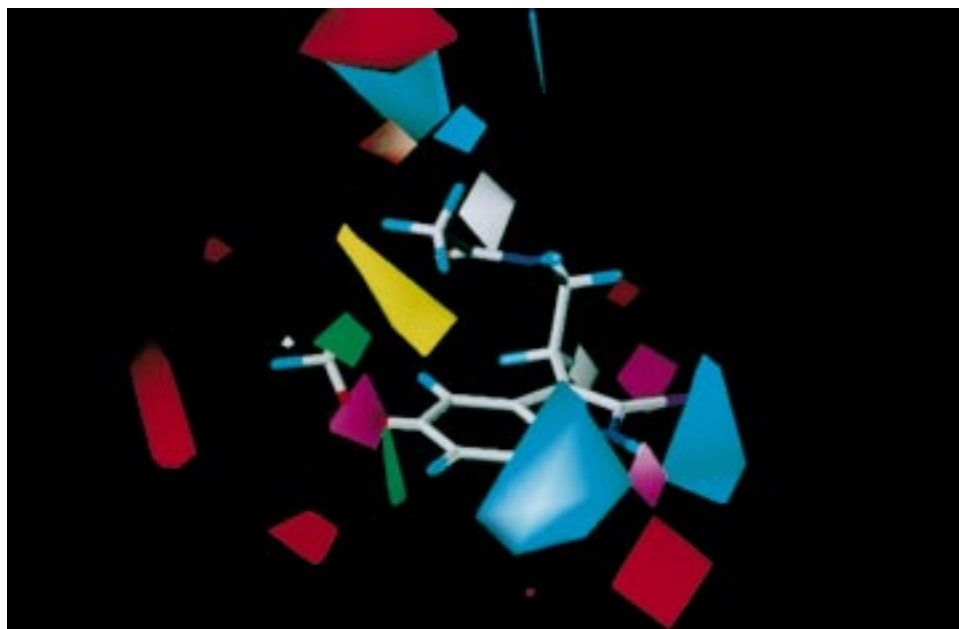
**Figure 14.** Electrostatic graphical results of PLS model G7 with 2-iodomelatonin (white = positive charge increase affinity; purple = negative charge increase affinity).



**Figure 15.** Lipophilic graphical results of PLS model G7 with 2-iodomelatonin (cyan = hydrophilicity increase affinity; yellow = lipophilicity increase affinity).

the CoMFA contour plot shows green colored regions where increased steric bulk is associated with enhanced affinity and red colored regions where increased steric bulk is associated with diminished affinity. The favorable steric region close to the end of the N-acyl chain agrees with the results of a SAR study previously reported by Depreux et al.<sup>13</sup> In Figure 14, regions where increased positive charge is favorable for affinity are indicated in white, while regions where increased negative charge is favorable for affinity are indicated in purple. The presence of a purple zone close to the methoxy group confirms the importance of the role played by the electronegative oxygen lone pairs in the melatonin receptor binding. The Figure 15 reveals

regions colored in yellow which correspond to a favorable influence of lipophilicity and regions colored in cyan which correspond to a favorable influence of hydrophilicity. The position of a yellow zone between the methoxy group and the end of the N-acyl chain suggests that this hydrophobic favorable influence may be related to the favorable influence of bulky nonpolar substituents in this region. Figure 16 summarizes all the significant statistical signals and shows the complexity for interpreting the steric, electrostatic, and lipophilic influences. Sicsic et al.<sup>18</sup> have previously reported a CoMFA model ( $n = 44$ ,  $q^2 = 0.80$ ,  $N = 5$ ,  $r^2 = 0.97$ ,  $s = 0.25$ ,  $F = 222$ ) with steric and electrostatic relative contributions, 52% and 48%, respectively. This model is statistically



**Figure 16.** Steric, electrostatic, and lipophilic graphical results of PLS model G7 with 2-iodomelatonin (red = steric decrease affinity; green = steric increase affinity; white = positive charge increase affinity; purple = negative charge increase affinity; cyan = hydrophilicity increase affinity; yellow = lipophilicity increase affinity).

**Table 20.** Experimental vs Predicted  $pIC_{50}$  Values for the Test Set of Model G7

compd	exptl value	predct value	gap value	compd	exptl value	predct value	gap value	compd	exptl value	predct value	gap value	compd	exptl value	predct value	gap value
65	4.5	4.7	0.2	85	5.8	8.0	2.2	104	7.0	7.3	0.3	124	7.8	8.1	0.3
66	4.8	5.1	0.3	86	5.8	5.3	0.5	105	7.0	7.4	0.4	125	7.8	7.6	0.2
67	4.8	5.1	0.3	86	5.8	5.3	0.5	106	7.1	7.7	0.6	126	7.9	8.6	0.7
68	4.9	5.1	0.2	87	5.9	6.0	0.1	107	7.1	7.7	0.6	127	8.0	8.1	0.1
69	5.0	4.4	0.6	88	6.0	6.8	0.8	108	7.1	6.9	0.2	128	8.1	8.3	0.2
70	5.0	5.1	0.1	89	6.0	7.7	1.7	109	7.2	7.8	0.6	129	8.1	7.7	0.4
71	5.0	6.7	1.7	90	6.1	7.1	1.0	110	7.3	8.0	0.7	130	8.2	7.5	0.8
72	5.0	6.5	1.5	91	6.2	7.6	1.4	111	7.3	7.5	0.2	131	8.3	7.2	1.1
73	5.0	6.4	1.4	92	6.2	6.7	0.5	112	7.3	6.5	0.8	132	8.3	9.4	1.1
74	5.1	5.7	0.6	93	6.3	7.1	0.8	113	7.3	7.7	0.4	133	8.4	8.5	0.1
75	5.2	5.8	0.6	94	6.3	6.2	0.1	114	7.4	7.8	0.5	134	8.4	8.2	0.2
76	5.2	6.2	1.0	95	6.3	6.2	0.1	115	7.4	8.0	0.6	135	8.5	8.5	0
77	5.4	6.4	1.0	96	6.3	6.5	0.2	116	7.4	8.0	0.6	136	8.7	7.6	1.1
78	5.5	6.2	0.7	97	6.5	6.1	0.4	117	7.4	7.0	0.4	137	8.9	7.7	1.2
79	5.5	5.7	0.2	98	6.5	6.4	0.2	118	7.4	7.4	0	138	8.9	7.8	1.1
80	5.6	6.4	0.8	99	6.7	7.7	1.0	119	7.4	8.4	1.0	139	9.0	8.4	0.6
81	5.6	6.4	0.8	100	6.8	8.1	1.3	120	7.6	7.9	0.3	140	9.0	9.2	0.2
82	5.7	5.6	0.1	101	6.8	7.3	0.5	121	7.6	7.2	0.4	141	9.0	9.0	0
83	5.7	6.6	0.9	102	6.8	7.1	0.3	122	7.7	8.0	0.3	142	9.5	8.6	0.9
84	5.8	7.7	1.9	103	6.9	7.0	0.1	123	7.7	6.3	1.4				

significant, but four compounds of the training set were excluded as outliers. For two of them, it would seem that the conformational freedom of their butyl substituent was not taken into account. On the other hand, our model is able to predict fairly the binding affinities for compounds presenting such substituents on the N-acyl chain.

**Validation of the CoMFA Model.** To validate our model, we have attempted to predict the affinities for the 78 ligands of the test set. The predicted  $pIC_{50}$  values for these 78 compounds of the test set as well as residual values are given in Table 20, and the results are graphically represented in Figures 11 and 12. The correlation coefficient  $r^2$  of this linear regression has a value of 0.66 in agreement with the  $q^2$  value (0.62) of the model. Fifty percent of compounds are predicted with a gap less than 0.5, while 82% of compounds are predicted with a gap less than 1. Our model did not predict accurately the  $pIC_{50}$  values for the compounds

**85** and **89**. The  $pIC_{50}$  predicted values for these compounds were overestimated with gap values respectively of 2.2 and 1.7. With regard to the size of our test set (78 compounds), these excessive values do not call the statistical validity of our model into question. On the other hand, these ligands present particular structural features not encountered in the training set. Compound **85** is the only one which shows the amidic function separated from the aromatic moiety with more than four links. In another way, compound **89** is the only one which exhibits no substituent at the end of the N-acyl chain. A useful model ought to be able to avoid the synthesis of compounds with very low or without affinity but must be able to advise the synthesis of all the virtual compounds with good affinity. The results of this test set can be used to verify if our model presents these characteristics. If, based upon the results of the prediction, the synthesis of all the products (31) with a predictive  $pIC_{50}$  lower than 7 would not be realized, the

gain in the synthesis step would be around 40% (31/78). No compound with good affinity would be lost (from these 31 ligands, only three have pIC<sub>50</sub> values higher than 7, 7.1, 7.3, and 7.7). Among the 47 synthesized products, 37 would have presented a good or low affinity (>7), 8 a very low affinity (between 6 and 7), and only 2 no affinity. This clearly shows the usefulness of our model.

## Conclusion

In summary, a set of structurally different ligands was used in the present study to define in the best way the geometry of the melatonin agonist receptor pharmacophore. This pharmacophoric assumption was then used as a basis to perform a CoMFA study and to generate in this way a 3D-QSAR agonist model. The predictive power of the proposed model was discerned by successfully testing a wide set of agonist compounds. Our model is very interesting since it can predict binding affinities for a wide panel of ligands for the sheep brain melatonin receptor considering steric, electrostatic, and lipophilic influences. It brings important structural insights to aid the design of novel melatonin-ergic agonist ligands prior to their synthesis. We are waiting to know the three-dimensional structure of the receptors before we perform docking experiments which would show the accuracy of our model.

**Acknowledgment.** We are specially grateful to E. Raimbaud, E. Jacobi, P. Depreux, and E. Vangrevelinghe for advice given on the subject.

## References

- Lerner, A. B.; Case, J. D.; Heinzelman, R. V. Structure of melatonin. *J. Am. Chem. Soc.* **1959**, *81*, 6084–6085.
- Miles, A.; Philbrick, D. R. S.; Thomson, C. *Melatonin: Clinical perspectives*; Oxford Medical Publications: Oxford University Press: Oxford, 1988.
- Cagnacci, A. Melatonin in relation to physiology in adult humans. *J. Pineal Res.* **1996**, *21*, 200–213.
- Brugger, P.; Marktl, W.; Herold, M. Impaired nocturnal secretion of melatonin in coronary heart disease. *Lancet* **1995**, *345*, 1408–1415.
- Reiter, R. J. Functional pleiotropy of the neurohormone melatonin: antioxidant protection and neuroendocrine regulation. *Front. Neuroendocrinol.* **1995**, *16*, 383–415.
- Reiter, R. J. Antioxidant actions of melatonin. *Adv. Pharmacol.* **1997**, *38*, 1103–117.
- Dawson, D.; Encel, N. Melatonin and sleep in humans. *J. Pineal Res.* **1993**, *15*, 1–12.
- Ebisawa, T.; Karne, S.; Lerner, M. R.; Reppert, S. M. Expression cloning of a high affinity melatonin receptor from *Xenopus* dermal melanophores. *Proc. Natl. Acad. Sci. U.S.A.* **1994**, *91*, 6133–6137.
- Reppert, S. M.; Weaver, D. R.; Godson, C. Melatonin receptors step into the light: cloning and classification of subtypes. *Trends Pharmacol. Sci.* **1996**, *17*, 100–102.
- Gaillard, P.; Carrupt, P. A.; Testa, B.; Schambel, P. Binding of arylpiperazines, (aryloxy)propalamines, and tetrahydropyridylindoles to the 5-HT<sub>1A</sub> receptor: Contribution of the molecular lipophilicity potential to three-dimensional quantitative structure-affinity relationship models. *J. Med. Chem.* **1996**, *39*, 126–134.
- Cramer, R. D. III; Patterson, D. E.; Bunce, J. D. Comparative molecular field analysis (CoMFA). 1. Effect of shape on binding of steroids to carrier proteins. *J. Am. Chem. Soc.* **1988**, *110*, 5959–5967.
- Yous, S.; Andrieux, J.; Howell, H. E.; Morgan, P.; Renard, P.; Pfeiffer, B.; Lesieur, D.; Guardiola-Lemaitre, B. Novel Naphthalenic Ligands with High Affinity for the Melatonin Receptor. *J. Med. Chem.* **1992**, *35*, 1484–1486.
- Depreux, P.; Lesieur, D.; Ait Mansour, H.; Morgan, P.; Howell, H. E.; Renard, P.; Caignard, D. H.; Pfeiffer, B.; Delagrance, P.; Guardiola, B.; Yous, S.; Demarque, A.; Adam, G.; Andrieux, J. Synthesis and Structure–Activity Relationships of Novel Naphthalenic and Bioisosteric Related Amidic Derivatives as Melatonin Receptor Ligands. *J. Med. Chem.* **1994**, *37*, 3231–3239.
- Langlois, M.; Brémont, B.; Shen, S.; Poncet, A.; Andrieux, J.; Sicsic, S.; Serraz, I.; Mathé-Allainmat, M.; Renard, P.; Delagrance, P. Design and Synthesis of New Naphthalenic Derivatives as Ligands for 2-[<sup>125</sup>I]IodoMelatonin Binding Site. *J. Med. Chem.* **1995**, *38*, 2050–2060.
- Garratt, P. J.; Travard, S.; Vonhoff, S. Mapping the Melatonin Receptor. 4. Comparison of the Binding Affinities of a Series of Substituted Phenylalkyl Amides. *J. Med. Chem.* **1996**, *39*, 1797–1805.
- Mathé-Allainmat, M.; Gaudy, F.; Sicsic, S.; Dangy-Caye, A. L.; Shen, S.; Brémont, B.; Benatalah, Z.; Langlois, M.; Renard, P.; Delagrance, P. Synthesis of 2-amido-2,3-dihydro-1H-phenalene Derivatives as New conformationally Restricted Ligands for Melatonin Receptor. *J. Med. Chem.* **1996**, *39*, 3089–3095.
- Leclerc, V.; Depreux, P.; Lesieur, D.; Caignard, D. H.; Renard, P.; Delagrance, P.; Guardiola-Lemaitre, B.; Morgan, P. Synthesis and Biological Activity of Conformationally Restricted Tricyclic Analogs of the Hormone Melatonin. *Bioorg. Med. Chem. Lett.* **1996**, *6*, 1071–1076.
- Sicsic, S.; Serraz, I.; Andrieux, J.; Brémont, B.; Mathé-Allainmat, M.; Poncet, A.; Shen, S.; Langlois, M. 3D Quantitative Structure–Activity Relationship of Melatonin Receptor Ligands: A Comparative Molecular Field Analysis Study. *J. Med. Chem.* **1997**, *40*, 739–748.
- Viaud, M. C.; Mamai, A.; Guerin, V.; Bennejean, C.; Renard, P.; Delagrance, P.; Guardiola-Lemaitre, B.; Howell, H. E.; Guillaumet, G. Substituted 3-amido and 3-amidoalkylbenzopyran Derivatives: Synthesis and Pharmacological Activity as Melatonin Ligands. *Pharm. Sci.*, submitted.
- Mazeas, D.; Viaud, M. C.; Guillaumet, G. Synthesis of Azaindolic Derivatives as Melatonin Analogs. Fourth European Conference of Groupement des Pharmacochimistes de l'Arc Atlantique, Glasgow (Ecosse), 10–11 September 1996.
- Morgan, P. J.; Lawson, M.; Davidson, G.; Howell, H. E. Melatonin inhibits cyclic AMP production in cultured ovine pars tuberalis cells. *J. Mol. Endocrinol.* **1989**, *5*, 3–8.
- Morgan, P. J.; Williams, L. M.; Davidson, G.; Lawson, M.; Howell, H. E. Melatonin receptors on ovine pars tuberalis: characterization and autoradiographical localization. *J. Neuroendocrinol.* **1989**, *1*, 1–4.
- SYBYL 6.2, Tripos Associates, Inc., St. Louis, MO.
- Clark, M.; Cramer, R. D., III; Van Opdenbosch, N. Validation of the General Purpose Tripos 5.2 Force Field. *J. Comput. Chem.* **1989**, *10*, 982–1012.
- Stewart, J. J. P. MOPAC: a semiempirical molecular orbital program. *J. Comput.-Aided Mol. Des.* **1990**, *4*, 1–103.
- Audry, E.; Dubost, J. P.; Dallet, P.; Langlois, M. H.; Colleter, J. C. The Molecular Lipophilic Potential: Application to a series of beta-adrenolytic amines. *Eur. J. Med. Chem.* **1989**, *24*, 155–161.
- (a) Gaillard, P.; Carrupt, P. A.; Testa, B.; Boudon, A. Molecular lipophilicity potential, a toll in 3D-QSAR. Method and Applications. *J. Comput.-Aided Mol. Des.* **1994**, *8*, 83–96. (b) Institut of medicinal Chemistry, University of Lausanne, BEP CH-1015 Lausanne, Switzerland.
- Simon, Z. Comparative molecular field analysis. Critical components. *Rev. Roum. Chim.* **1992**, *37*, 323–325.
- Folkers, G.; Merz, A.; Rogman, D. CoMFA: scope and limitations. In *3D QSAR in Drug Design. Theory Methods and Applications*; Kubinyi, H., Ed.; ESCOM Science Publishers: Leiden, 1993; pp 593–618.
- Van de Waterbeemd, H.; Testa, B. The parametrization of lipophilicity and other structural properties in drug design. In *Advances in Drug Research*; Testa, B., Ed.; Academic Press: London, 1987; Vol. 16, pp 87–227.
- Spadoni, G.; Balsamini, C.; Diamantini, G.; Di Giacomo, B.; Tarzia, G. Conformationally Restrained Melatonin Analogues: Synthesis, Binding Affinity for the Melatonin Receptor, Evaluation of the Biological Activity and Molecular Modeling Study. *J. Med. Chem.* **1997**, *40*, 1990–2002.